ORIGINAL ARTICLE

Future gamma-ray missions' polarimetric prospects

A. F. V. Cortez[1,2] · R. M. Curado da Silva[1,2] ⓘ · G. Rodriguez[3] · P. Cumani[4,5] ·
A. Morselli[3] · M. Hernanz[4] · V. Tatischeff[5] · M. Moita[1,2] · J. M. Maia[1,6] ·
P. Von Ballmoos[7] · A. Zoglauer[8]

© Springer Nature B.V. 2019

Abstract

High-energy astrophysics polarimetry may significantly benefit from e-ASTROGAM and from AMEGO mission proposals, since to date limited polarimetric measurements were performed in this domain, exclusively under 1 MeV. The polarimetric potential of both missions was analyzed in the Compton regime by Monte Carlo mass model simulations with MEGAlib toolkit. The performance of e-ASTROGAM was analyzed by simulating Si tracker and calorimeter alternative configurations and detection materials, within missions' volume, mass and power margins. The modulation polarimetric factor, Q, and the MDP were calculated for different polarized source types and for variable incidence angle measurement conditions. Finally, the polarimetric performances of both instruments was compared and analyzed. Q modulation factors obtained ranged between ~0.2 and ~0.4 in the 0.2–2.0 MeV band and MDP ~0.65% was estimated for a 100% polarized Crab type source, 1 Ms. observation time and 3σ significance.

✉ R. M. Curado da Silva
rui.silva@coimbra.lip.pt

1   Laboratório de Instrumentação e Física Experimental de Partículas, Coimbra, Portugal

2   Department of Physics, University of Coimbra, Coimbra, Portugal

3   INFN Roma Tor Vergata, via della Ricerca Scientifica 1, I-00133 Rome, Italy

4   ICE-CSIC/IEEC, Campus UAB, 08193 Bellaterra, Barcelona, Spain

5   CSNSM, IN2P3-CNRS and Univ Paris-Sud, F-91405 Orsay Cedex, France

6   Department of Physics, University of Beira-Interior, Covilhã, Portugal

7   IRAP, 9, av. du Colonel-Roche, 31028 Toulouse, France

8   Space Sciences Laboratory, University of California, Berkeley, CA 94720, USA

1 Introduction

The observation of two simultaneous signatures, a gravitational wave and a gamma-ray burst (GRB), emitted by a neutron star merger, has opened a new knowledge window: the multi-messenger astrophysics [1]. This new scientific field requires collaboration and coordination between different types of observational methods and different research communities. Gravitational waves' observation in ground facilities, such as LIGO-Virgo [2], coordinated with observations performed in gamma-ray space-based observatories will be essential in the multi-messenger era astrophysics, since GRBs provide useful constraints on the gravitational wave source localization. In this unique context, gamma-ray polarimetry may contribute to a wider understanding of γ-ray sources, such as pulsars, solar flares, active galactic nuclei, galactic black holes, and particularly GRBs [3, 4]. Measuring the polarization will provide two additional observational parameters: the polarization angle and the level of linear polarization. For some types of sources like pulsars, these additional parameters may allow better discrimination between different emission models characterizing the same object.

However, due to its complexity, no dedicated gamma-ray polarimeters are operating in space. Up to now, in the soft γ-ray domain (0.1–1 MeV), only a limited number of polarimetric measurements were performed by space instruments. SPI and IBIS instruments, on-board the INTEGRAL mission [5], provided statistically significant polarization observations on the Crab Pulsar, on the galactic black hole Cygnus X-1 and on some strong GRBs [6–9]. GAP (Gamma-Ray Burst Polarimeter), on IKAROS solar sail, measured the polarization of the GRB100826A [10]. POLAR onboard China's Tiangong-2 space laboratory performed detailed polarization measurements of the prompt emission of five GRBs [11].

The next generation of high-energy space telescopes should provide polarimetry, spectroscopy, timing, and imaging capabilities, such as e-ASTROGAM (enhanced ASTROGAM) and AMEGO (All-sky Medium Energy Gamma-ray Observatory) [12, 13] mission proposals. The e-ASTROGAM mission concept was submitted to ESA's Cosmic Vision M5 call. AMEGO is an international mission concept under development between NASA and european partners. The referred mission concepts share design similitudes such as Double-sided Silicon Strip Detector (DSSD) trackers and CsI calorimeters, however AMEGO includes a CZT calorimeter (Fig. 1). While e-ASTROGAM is foreseen to operate in the 0.3 MeV up to 3 GeV energy band, AMEGO should observe the sky in the 0.2 MeV-10 GeV band. In the framework of EU AHEAD project, e-ASTROGAM polarimetric potential was analyzed under different instrument configurations. Moreover, its baseline polarimetric performances was comparatively analyzed with AMEGO polarimetric potential.

2 e-ASTROGAM polarimetric performances

The polarimetric potential of the e-ASTROGAM mission proposal was analyzed by mass model simulation with MEGAlib simulation tool [14] for different tracker and calorimeter configurations (x, y and z dimensions, number of layers, spacing between layers, etc.), as well as for alternative detector types (scintillators and semiconductors), within the mission mass and power limits. Different source types were modelized on-
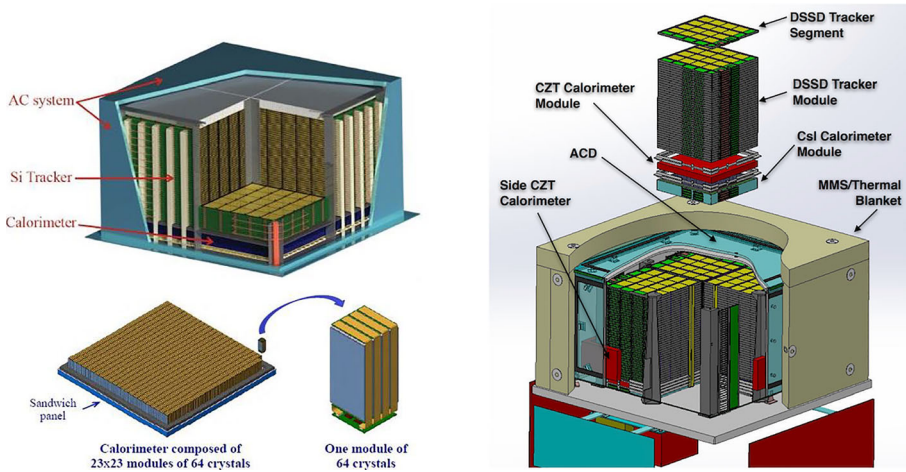
Fig. 1 Scientific payload overview of e-ASTROGAM (left) and AMEGO (right) mission proposals. Both instruments are composed by a DSSD Tracker, a Calorimeter and an Anticoincidence system, however with different configurations and detection materials

and off-axis. The polarimetric analysis was based exclusively in Compton events, since up to date no pair production experimental measurements where performed to validate simulation polarimetric models. Our main objective was to analyze the response of intrinsic performance of the instrument, given by the modulation factor, to the alternative configuration solutions. The MDP was calculated for more representative cases, since it takes into account complex external factors such as background, source flux and techniques to improve signal to noise ratio, like MEGAlib tool for event reconstruction.

2.1 Compton polarimetry

A polarized photon beam scattered by a detector element generates Compton scattered photons whose azimuthal distribution is modulated. Indeed, the scattered photons' angular direction depends on its initial polarization angle. If the scattered photon undergoes through a new interaction inside the detector, the statistical distribution of the photons' angular directions defined by the two interactions (double-event) provides a modulation curve whose degree and polarization direction of the incident beam can be measured. The azimuthal angular distribution of the scattered photons is given by the Klein-Nishina differential cross-section for linearly polarized photons:

$$\frac{d\sigma_{KN,P}}{d\Omega} = \frac{r_0^2}{2} \left(\frac{E'}{E}\right)^2 \left[\frac{E'}{E} + \frac{E}{E'} - 2sin^2\theta cos^2\phi\right], \tag{1}$$

where r_0 is the classical electron radius, E and E' are, respectively, the energies of the incoming and outgoing photons, θ the angle of the scattered photons and ϕ is the angle between the scattering plane and incident polarization plane.

The polarimetric performance of an instrument can be evaluated by calculating the polarimetric modulation factor, Q, of double-event distribution generated by a 100% polarized beam, and is defined as the amplitude of the modulation curve:

$$Q = \frac{d\sigma\left(\phi_{//}\right) - d\sigma(\phi_{\perp})}{d\sigma\left(\phi_{//}\right) + d\sigma(\phi_{\perp})}, \tag{2}$$

where $d\sigma(\phi_{//})$ and $d\sigma(\phi_{\perp})$, are the double-events over two orthogonal directions defined over the detector plane along the maxima and minima of the modulation curve.

For a given polarimeter the Minimum Detectable Polarization (MDP), for a space polarimeter in a background noise environment with 99% (3σ significance) confidence level [15], is given by:

$$MDP_{99\%} = \frac{4.29}{A \cdot \varepsilon \cdot S_F \cdot Q_{100}} \sqrt{\frac{A \cdot \varepsilon \cdot S_F + B}{\Delta T}} \tag{3}$$

where Q_{100} is the modulation factor for a 100% polarized source, ε the double event detection efficiency, A the polarimeter detection area in cm^2, S_F the source flux (photons·s^{-1}·cm^{-2}), B is the background count rate (counts/s) and ΔT the observation time in seconds.

2.2 e-ASTROGAM baseline polarimetric performances

In the framework of AHEAD Work Package 9 activities, e-ASTROGAM baseline configuration (Table 1) was simulated in order to estimate its polarimetric potential for a 100% polarized Crab source type emission in two energy bands: a low energy band, from 0.2 MeV up to 2.0 MeV and a high energy band, between 0.8 MeV and 5.0 MeV. The beam profile was based on a Crab type far-field point source and the data obtained resulted from 500,000 triggers in the sensitive detection material. Each trigger was generated when at least 2 interactions occurred in distinct pixels. As can be seen in Fig. 2, the integrated modulation in the 0.2–2.0 MeV band varies between 0.34 and 0.23, for a beam incidence angle between 0° and 90°. In the 0.8–5.0 MeV the integrated modulation factor varies between 0.25 and 0.16, between 0° and 90°. The calculated Q obtained for each band can be explained by previous simulation and experimental work [16, 17]. Actually, the modulation factor peaks for Compton photon scattering angles close to 90° (in the band Between ~200 and ~400 keV). Then it decreases dramatically

Table 1 e-ASTROGAM baseline configuration main simulation parameters

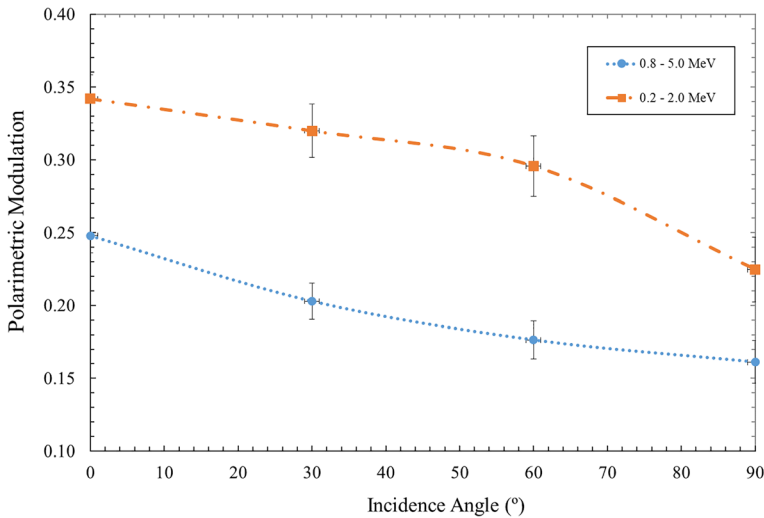| Si Tracker	DSSD layers' thickness (μm)	Number of layers	Inter-layer spacing (cm)
	500	56	1
CsI Calorimeter	Crystals' pitch (cm)	Lateral size (cm)	Thickness (cm)
	0.02	0.3	8

Fig. 2 e-ASTROGAM modulation factor for a Crab type far-field point source under variable beam incidence angles simulated for two different energy ranges: 0.2–2.0 MeV and 0.8–5.0 MeV

when the average scattering angles becomes increasingly lower for higher source photons' energies. The observed modulation degradation with the incidence angle is also in agreement with previous simulation and experimental studies [16–19]. In fact, an off-axis beam generates a double-event distribution in the neighboring pixels which reflects not only the polarization status of the beam but as well its angular offset with respect to the normal incidence direction. Depending on the beam linear polarization angle, it combines with the incidence angle to amplify or to smooth the effects generated in the modulation of double-events as show in [16] simulation analysis and in [17] experimental work. For simplicity, we simulated beam polarization angle aligned with instruments' main axis (X and Y) since the variations in the expected results (related with orientation angle and with pixel shape in small scale) obtained for other angle orientations would not change configuration optimization's conclusions, as shown in the same publications.

The calculated MDP for e-ASTROGAM in the 0.2–2.0 MeV energy range, under the referred conditions, was 0.65% for a Crab like source and a photonic background (cosmic and atmospheric, which dominant in this band), for 1 Ms. observation time. For the Galactic Centre emission profile, MDP of 10.8% was calculated for a 10 mCrab flux, in the 0.2–2.0 MeV energy range and 1-year observation time. These MDP estimations meet comfortably e-ASTROGAM mission requirements: MDP < 20% for a 10 mCrab source flux and 1-year observation time, in the 0.3–2.0 MeV energy range.

2.3 Si tracker

After e-ASTROGAM's baseline analysis, the modulation polarization factor was calculated for different Si tracker configurations (variable number of layers, variable spacing and variable Si layer thickness) within mission's operational limits. The simulated source was a power law (2.0) emission profile, far-field point source in the 0.5–2 MeV energy range between, for 500,000 triggers generated within the sensitive

volume. Table 2 summarizes the simulation sets performed. The modulation factors obtained for each Si tracker configuration per simulation set are presented in Fig. 3. In Simulation Set 1, the spacing between layers was maintained constant, while varying the layer thickness and the number of layers. In Simulation Set 2 the sensitive volume was constant and in Set 3 the number of layers was unchanged. The obtained curve shape (top right Fig. 3) was determined by two factors: i) thinner layers provide better modulation due to higher double-event fraction near 90°, therefore modulation decreases with layers' thickness; ii) modulation factor improves with the distance between the two interactions forming a double-event. Although the sensitive volume was kept constant, the overall tracker volume was variable (within the baseline volume), varying, as well, the average double-event distance and therefore the modulation. The results obtained show that e-ASTROGAM Si Tracker original configuration performances are generally the best performant configurations within the mission limits (999 kg and 1340 W total payload mass and power, respectively). Moreover, the dependence on the geometric parameters within the limits established was small. The alternative configurations including more detection elements did not provide a substantial performance increase. In fact, Simulation Set 2 (right Fig. 3) performed under constant sensitive volume conditions, provides a clear picture of modulation dependence on the number of channels. On the same sense, the configurations with a lower pixelization level did not decrease distinctly the polarization modulation. The MDP was calculated for configuration cases when distance between layers and pixels, and therefore double-event profiles trajectories, change more significantly (in simulation set 1 and 2), for the same sensitive volume. The MDP obtained ranged between 0.61% (near e-ASTROGAM configuration) and 2.3% (30 layers). Each configuration was simulated under the same background environment. For each configuration the trajectory reconstruction simulation tool provided an improved signal-to-noise ratio dependent on the trajectory resolution of each configuration. Generally, the larger the distance between elements, the better the reconstruction tool improves signal-to-noise ratio and, therefore, better MDP is obtained.

In order to obtain a net performance improvement, it would be necessary to change radically the configuration or the detection volume, which would probably not fit within mission operational limits established for the M5 ESA Call. However, these results show that a similar instrument with a lower number of detection elements, therefore with less channels, less electronics and therefore lower complexity would provide polarimetric performances of the same order. When designing a mission that should address polarimetric measurements, this conclusion is particularly useful in order to build simpler instruments with lower number of channels.

Table 2 e-ASTROGAM Si Tracker simulation main parameters for a 100% polarized, normal, Far-Field Point, power law Source in the 0.5–2.0 MeV range

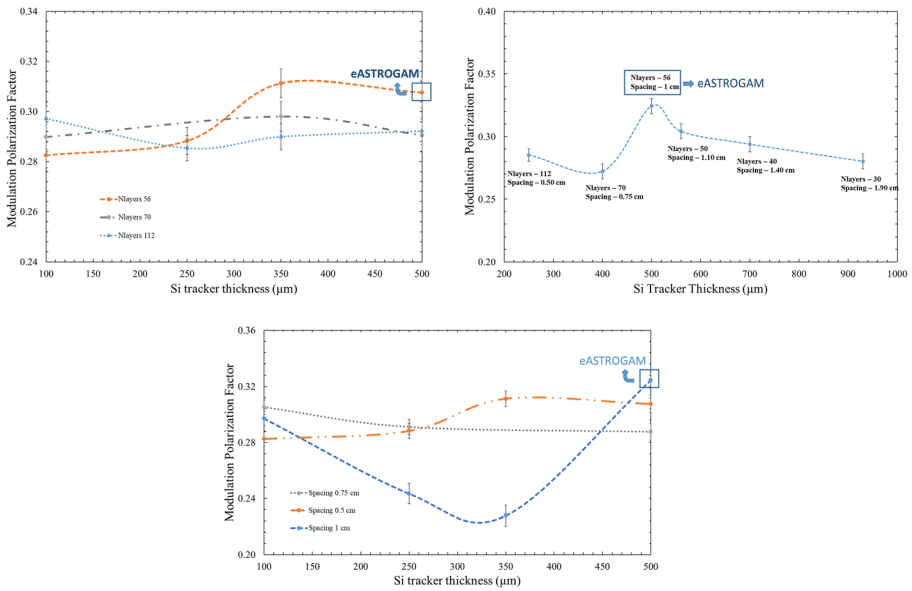| Simulation set	Thickness (μm)	Number of layers	Inter-layer spacing (cm)	Sensitive volume
1	100–500	56, 70, 112	Constant = 1	Variable
2	250–950	30–112	0.50–1.90	Constant
3	100–500	Constant = 56	0.5–1.0	Variable

Fig. 3 The e-ASTROGAM tracker modulation polarization factor for different configurations: (top left) total Si tracker inter-layer spacing was set constant; (top right) Si tracker sensitive volume was set constant; (bottom) total Si tracker number of layers was set constant. The e-ASTROGAM baseline configuration estimated modulation is indicated in each graphic

2.4 Calorimeter

With the objective to study calorimeter alternative solutions, further simulations were performed for CZT and CdTe detection materials. Their performances were compared with CsI calorimeter e-ASTROGAM baseline configuration. The simulated source was a far-field point within an energy range up to 3 MeV, for 500,000 triggers and different incidence angles: 0°, 30°, 60° and 90°. Right Fig. 4 shows that potentially a calorimeter based on CdTe performs better than a CsI calorimeter for a power law (2.0) in the 0.5–2.0 MeV range. However, the CdTe/CZT simulation configuration is not realistic since it is not possible to grow 8 cm CdTe/CZT crystals with fine detection properties. A realistic configuration would require a crystal segmentation below 10 mm thickness.
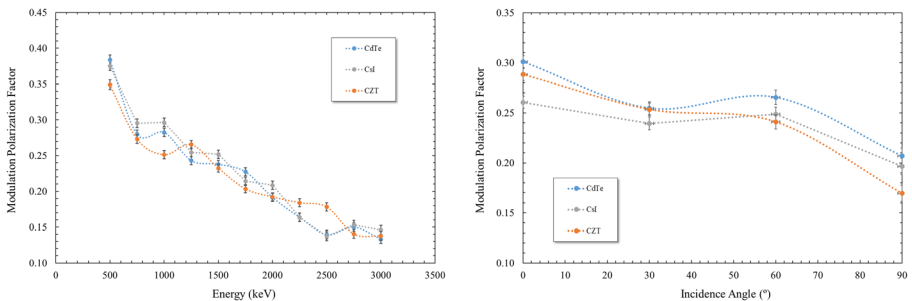

Fig. 4 The polarization modulation factor for distinct e-ASTROGAM calorimeter materials (CsI, CdTe and CZT): (left) in the energy band between 0.5 and 3.0 MeV; (right) for variable source emissions' incidence angles for a power law emission profile

This configuration would increase the number of channels, but it would improve the calorimeter intrinsic Q factor, since increased segmentation resolves better the double events trajectory. Therefore, the CdTe/CZT modulation obtained can be considered as a lower limit estimation. Its better efficiency and better energy resolution are the main factors that explain the better modulation obtained when comparing with CsI baseline configuration. Left Fig. 4 represents the modulation for monochromatic beams in the 0.5–3.0 MeV energy range. However, the modulation obtained for each material is not clearly distinct, especially in the energy range between 1.0 and 1.5 MeV, where lays an inflection in the materials' attenuation curve as pair production becomes active. CsI provides a slightly higher fraction of Compton events than CZT in the pair region, which explains the shape of the curve between 1 MeV and 1.5 MeV.

Subsequently, alternative configurations of calorimeter were analyzed. The pitch between voxels, the side X-Y voxels size and the crystal thickness were changed in a range of combinations shown in Table 3. The obtained results are represented in Fig. 5. Smaller crystals (6 cm) improve the calorimeter modulation factor, since better modulation factor is obtained for Compton scattering angles near 90°. For thinner crystals, a greater ratio of near 90° scattering angles are generated inside the calorimeter. The same ~90° scattering angle ratio explain why the wider pitch solution performs better (Fig. 5). Although Simulation Set 5 (Fig. 5 bottom left) is not so easy to interpret, we can at least conclude that smaller lateral size voxels (0.3 and 0.4 cm) perform slightly better than larger ones. In fact, wider X-Y lateral size voxels stop a bigger percentage of double-events within the irradiated pixel and therefore the double-event recorded in the surrounding voxels decreases and, consequently, also the modulation.

Comparing the level of geometric changes between the tracker and the calorimeter (the calorimeter volume was reduced by 75% of instrument baseline), we verified that the tracker contribution for overall polarization modulation is dominant. Smaller geometric changes in the tracker show a higher level of impact in the polarimetric performances. Therefore, if a geometric configuration modification should be implemented in the instrument to improve its polarimetric performance, it should be given priority to the tracker. Nevertheless, this set of simulations shows that there are valid alternative calorimeter materials that can improve by ~10 to 20% the instrument modulation.

Table 3 e-ASTROGAM calorimeter simulation main parameters for a 100% polarized, normal, Far-Field Point Source

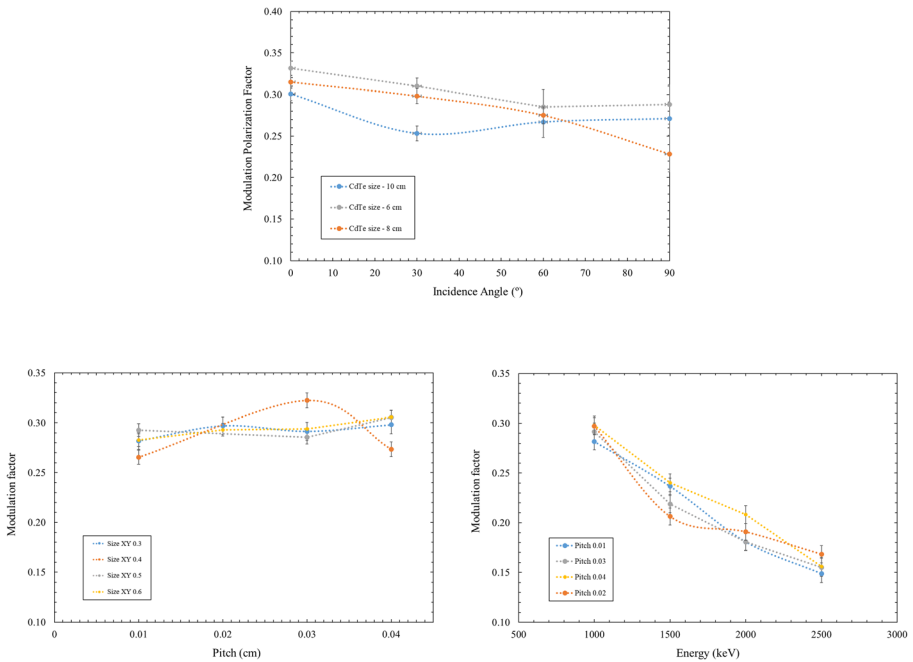| Simulation set	Crystal pitch (cm)	Lateral size (cm)	Crystal thickness (cm)	Material	Energy (MeV)
1	0.02	0.3	8	CsI, CdTe, CZT	0.5–3.0 monoenergetic
2	0.02	0.3	8	CsI, CdTe, CZT	0.5–2.0 power law (2.0)
3	0.02	0.3	6–10	CdTe	0.5–2.0 power law (2.0)
4	0.1–0.4	0.3	8	CsI	1–2.5 monoenergetic
5	0.1–0.4	0.3–0.6	8	CsI	0.5–2.0 power law (2.0)

Fig. 5 The polarization modulation factor when varying different e-ASTROGAM calorimeter configuration parameters: (top) CdTe crystal thickness; (bottom left) CsI crystals' lateral size and pitch; (bottom right) CsI crystals' pitch

3 AMEGO and e-ASTROGAM compared polarimetric performances

The polarimetric performances of both mission proposals, AMEGO and e-ASTROGAM, were simulated and compared under the same environment simulation conditions (background, emission source, pointing, etc.). Although, the instrument concepts of both missions are relatively similar (Fig. 1), the most significant design differences are: i) Si tracker DSSD array dimensions (5×5 in the case of e-ASTROGAM and 4×4 in AMEGO); ii) Si tracker number of layers (e-ASTROGAM: 56 layers; AMEGO: 60 layers); iii) calorimeter composition (CsI for e-ASTROGAM and CZT + CsI for AMEGO).

The modulation factor obtained for each instrument mass model, simulated with MEGAlib, is represented in Fig. 6. The modulation factor obtained for e-ASTROGAM under 100% polarized monochromatic, far-field point sources in the 0.25–2.5 MeV energy range is slightly better than AMEGO's modulation. This difference can be explained by the superior number of Si elements of the e-ASTROGAM tracker (5×5 DSSD arrays). A larger number of Si elements in X and Y instrument axis generates more near-90° scattering angles, improving modulation resolution [16, 18]. Instead, AMEGO superior number of layers (in Z) do not influence the modulation in the same measure, since for low scattering angles the intrinsic modulation of double-events' distribution is significantly lower when compared with near-90° scattering angles. In spite of AMEGO advantage provided by the calorimeter CZT (see section 2 d), its impact in the instrument performance is not significant, since the contribution of the Si
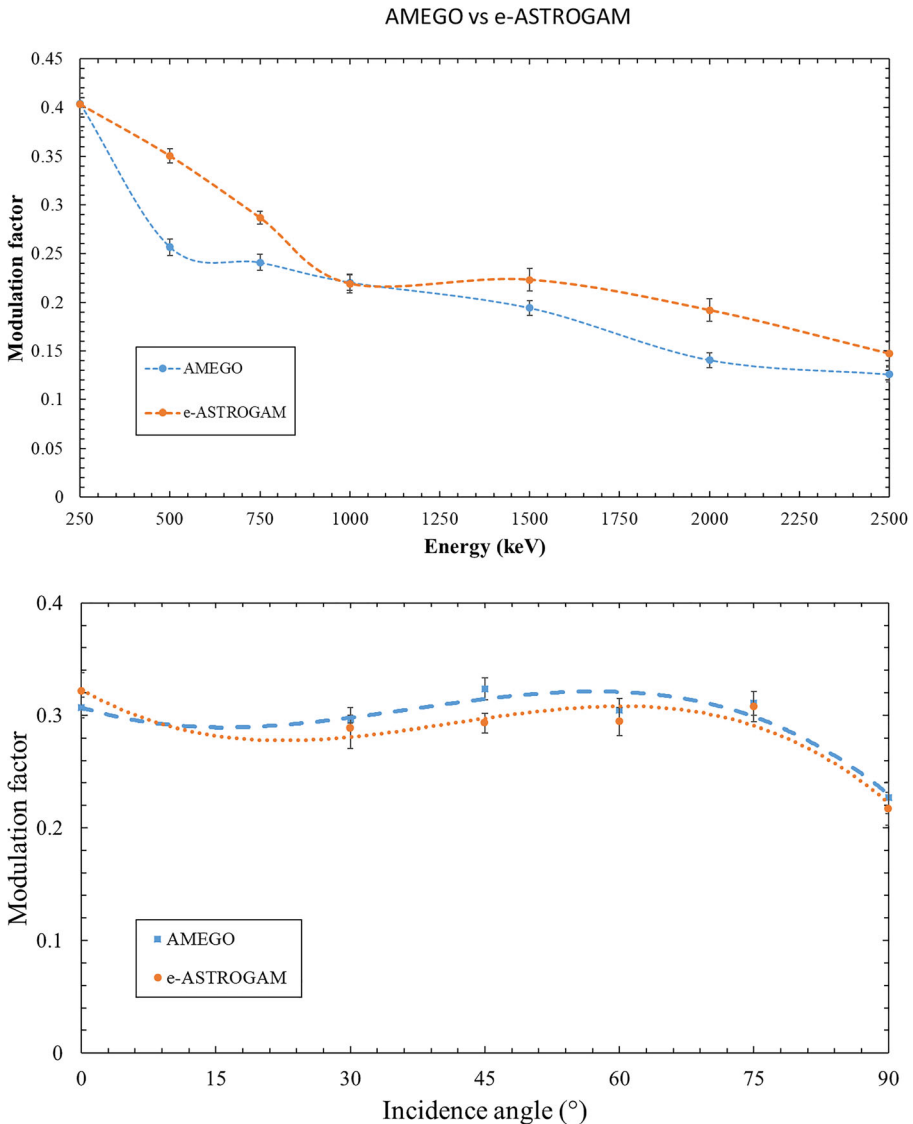
Fig. 6 AMEGO vs e-ASTROGAM polarization modulation as a function of the energy (top) and of the incidence angle (bottom), for a Crab type source in the 0.2–2.0 MeV energy range

tracker of both instruments for overall polarization is dominant. The set of simulations performed for a Crab type source in the 0.2–2 MeV energy range shows a slightly better modulation factor for e-ASTROGAM at normal incidence angles. For incidence angles up to 90°, AMEGO performed better, which can be explained by the lateral CZT elements that play a more relevant role in the case of off-axis incidence angles.

The MDP estimated, for a Crab source type, 3σ, 1 Ms. observation time and a photonic background in the 0.2–2.0 MeV energy range, was: 0.65% for e-ASTROGAM and 0.66% for AMEGO mission. Both MDPs are below 1% polarization detection level and are practically equivalent. Therefore, e-ASTROGAM better

modulation should not necessarily mean better MDP of the same other, since better efficiency (more Si layers and CsI + CZT calorimeter) and better background rejection (side CZT) are provided by AMEGO configuration. Furthermore, AMEGO Si tracker lower number of channels is an advantage when launch costs and complexity must be considered, which can be a better alternative if the polarimetric sensitivity is almost equivalent to other concepts.

4 Conclusions

In the framework of EU AHEAD project, e-ASTROGAM polarimetric performances were studied and analyzed by instrument mass model simulation. The integrated modulation in the 0.2–2.0 MeV band is 0.34 for a normal, 100% polarized beam. The respective MDP is 10.8% for a 10 mCrab flux and 1-year observation time, meeting MDP the mission requirements (< 20%). Furthermore, the results obtained helped to understand how the different geometry parameters influence the polarimetric performances of the instrument. The e-ASTROGAM Si Tracker original configuration compared with alternative configurations generically presents the best polarimetric performances within the mission limits. Furthermore, the configurations with a lower pixelization level did not decrease significantly the polarization modulation, therefore a simpler and lower number of channels' instrument configuration can be a fine option when complexity and number of channels are an issue. Simulations showed that CdTe calorimeter performed better as a polarimeter than a CsI calorimeter, mainly due to its better energy resolution and efficiency. The polarization modulation factor obtained for e-ASTROGAM in the energy range between 1 MeV and 2.5 MeV is slightly better than AMEGO's polarimetric performances. Nevertheless, MDP performances of the two missions are almost equivalent. Therefore, AMEGO less number channels and lower tracker complexity becomes an interesting advantage.

References

1. Goldstein, A., Veres, P., Burns, E., et al.:An Ordinary Short Gamma-Ray Burst with Extraordinary Implications: Fermi-GBM Detection of GRB 170817A. Astrophys. J. Lett. **848**, L14 (2017a)
2. The LIGO Scientific Collaboration and the Virgo Collaboration. GCN Circ. 21505, 2017-08-17
3. Lei, et al.: Compton polarimetry in gamma-ray astronomy. Space Sci. Rev. **82**, 309–388 (1997)
4. Bellazzini, R., et al.: X-ray polarimetry: A new window in astrophysics, eds. Cambridge University Press, (2010)
5. Winkler, C., Courvoisier, T.J.-L., Di Cocco, G., Gehrels, N., Giménez, A., Grebenev, S., Hermsen, W., Mas-Hesse, J.M., Lebrun, F., Lund, N., et al.: The Integral Mission. Astron. Astrophys. **411**, L1–L6 (2003)
6. Dean, A.J., Clark, D.J., Stephen, J.B., McBride, V.A., Bassani, L., Bazzano, A., Bird, A.J., Hill, A.B., Shaw, S.E., Ubertini, P.: Polarized gamma ray emission from the CRAB. Science. **321**, 1183–1185 (2008)
7. Forot, M., Laurent, P., Grenier, I.A., Gouiffès, C., Lebrun, F.: Polarization of the Crab pulsar and nebula as observed by the INTEGRAL/IBIS telescope. Astrophys. J. **688**, L29 (2008)

8. Laurent, P., Rodriguez, J., Wilms, J., Cadolle Bel, M., Pottschmidt, K., Grinber, V.: Polarized gamma-ray emission from the galactic black hole Cygnus X-1. Science. **332**, 438–439 (2011)

9. Götz, D., Laurent, P., Lebrun, F., Daigne, F., Bošnjak, Ž., et al.: Variable polarization measured in the prompt emission of GRB 041219A using IBIS on board INTEGRAL. Astrophys. J. Lett. **695**, L208 (2009)

10. Yonetoku, D., Murakami, T., Gunji, S., et al.: Detection of gamma-ray polarization in prompt emission of GRB 100826A. Astrophys. J. **743**, L30 (2011)

11. Zhang, S-N, Kole, M., et al.: Detailed polarization measurements of the 5 GRB prompt emission by POLAR, Nature Astronomy, (2019)

12. Angelis, D., et al.: The e-ASTROGAM mission: exploring the extreme universe with gamma rays in the MeV - GeV range. Exp. Astron. **44**(1), 25 (2017)

13. Moiseev, A., et al.: All-sky medium energy gamma-ray observatory (AMEGO), ICRC2017, PoS, **301**, 798

14. Zoglauer, et al.: MEGAlib – the medium energy gamma-ray astronomy library. New Astron. Rev. **50**, 629–632 (2006)

15. Weisskopf, M.C., Elsner, R.F., O'Dell, S.L.: On understanding the figures of merit for detection and measurement of x-ray polarization, Proc. SPIE 7732, Space Telescopes and Instrumentation 2010: Ultraviolet to Gamma Ray, 77320E (29 July 2010)

16. da Silva, R.M.C., Caroli, E., Stephen, J.B., Siffert, P.: CIPHER, a polarimeter telescope concept for hard X-ray astronomy. Exp. Astron. **15**(1), 45–65 (2003)

17. Curado da Silva, R.M., Auricchio, N., Caroli, E., et al.: Polarimetry study with a CdZnTe focal plane detector. IEEE Trans. Nucl. Sci. **58**(4), 2118–2123 (2011)

18. Curado da Silva, R.M., Caroli, E., Stephen, J.B.: Polarization degree and direction angle effects on a CdZnTe focal plane performance. IEEE Trans. Nucl. Sci. **59**(4), 1628–1635 (2012)

19. Moita, M., Caroli, E., Maia, J.M., et al.: Compton polarimetry with a multi-layer CdTe focal plane prototype. Nucl. Instr. Meth. A. **918**, 93–98 (2019)